



Molecular Crystals and Liquid Crystals Science and Technology. Section A. Molecular Crystals and Liquid Crystals

Publication details, including instructions for authors and subscription information:

<http://www.tandfonline.com/loi/gmcl19>

Molecular Metals Based on Nonplanar Donor BEDT-ATD: Appearance of Metal-Insulator Transition by Anion or Solvent Replacement

Kenichi Imaeda ^a, Jonas Kröber ^a, Chikako Nakano ^a, Masaaki Tomura ^a,
Shoji Tanaka ^a, Yoshiro Yamashita ^a, Hayao Kobayashi ^a, Hiroo
Inokuchi ^a & Akiko Kobayashi ^b

^a Institute for Molecular Science, Myodaiji, Okazaki, 444, Japan

^b Department of Chemistry, Faculty of Science, The University of Tokyo,
Hongo, Bunkyo-ku, Tokyo, 113, Japan

Version of record first published: 24 Sep 2006

To cite this article: Kenichi Imaeda, Jonas Kröber, Chikako Nakano, Masaaki Tomura, Shoji Tanaka, Yoshiro Yamashita, Hayao Kobayashi, Hiroo Inokuchi & Akiko Kobayashi (1997): Molecular Metals Based on Nonplanar Donor BEDT-ATD: Appearance of Metal-Insulator Transition by Anion or Solvent Replacement, Molecular Crystals and Liquid Crystals Science and Technology. Section A. Molecular Crystals and Liquid Crystals, 296:1, 205-216

To link to this article: <http://dx.doi.org/10.1080/10587259708032322>

PLEASE SCROLL DOWN FOR ARTICLE

Full terms and conditions of use: <http://www.tandfonline.com/page/terms-and-conditions>

This article may be used for research, teaching, and private study purposes. Any substantial or systematic reproduction, redistribution, reselling, loan, sub-licensing, systematic supply, or distribution in any form to anyone is expressly forbidden.

The publisher does not give any warranty express or implied or make any representation that the contents will be complete or accurate or up to date. The accuracy of any instructions, formulae, and drug doses should be independently verified with primary sources. The publisher shall not be liable for any loss, actions, claims, proceedings, demand, or costs or damages whatsoever or howsoever caused arising directly or indirectly in connection with or arising out of the use of this material.

MOLECULAR METALS BASED ON NONPLANAR DONOR BEDT-ATD:
APPEARANCE OF METAL-INSULATOR TRANSITION BY ANION OR
SOLVENT REPLACEMENT

KENICHI IMAEDA, JONAS KRÖBER, CHIKAKO NAKANO,
MASAAKI TOMURA, SHOJI TANAKA, YOSHIRO YAMASHITA,
HAYAO KOBAYASHI AND HIROO INOKUCHI
Institute for Molecular Science, Myodaiji, Okazaki 444, Japan

AKIKO KOBAYASHI
*Department of Chemistry, Faculty of Science, The University of Tokyo,
Hongo, Bunkyo-ku, Tokyo 113, Japan*

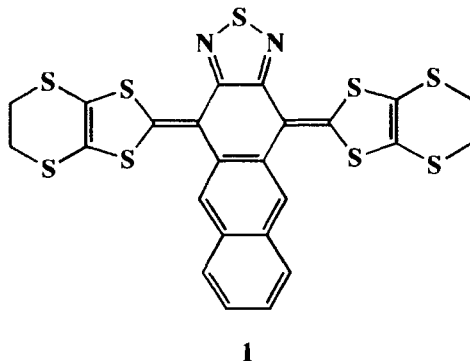
(Received 1 July 1996; In final form 17 September 1996)

Abstract We have prepared the cation radical salts based on a nonplanar donor 4,11-bis(4',5'-ethylenedithio-1',3'-dithiole-2'-ylidene)-4,11-dihydroanthra[2,3-c][1,2,5] thiadiazole (BEDT-ATD), (BEDT-ATD)₂X(Solvent) (X=PF₆, BF₄; Solvent=THF, DHF (2,5-dihydrofuran)). The band structure of a stable organic metal (BEDT-ATD)₂PF₆(THF) is presented. The replacement of an anion or a solvent molecule has induced a metal-insulator transition at 200 K and 150 K for (BEDT-ATD)₂BF₄(THF) and (BEDT-ATD)₂PF₆(DHF), respectively.

Keywords: *BEDT-ATD, cation radical salt, organic metal, band structure, metal-insulator transition*

INTRODUCTION

The search for a donor or an acceptor molecule with a small on-site Coulomb repulsion (*U*) is important to find new organic metals. 4,11-Bis(4',5'-ethylenedithio-1',3'-



dithiole-2'-ylidene)-4,11-dihydroanthra[2,3-c][1,2,5]-thiadiazole (BEDT-ATD, **1**) is a novel donor with a small U , showing a cyclic voltammogram with a small ΔE of 90 mV where ΔE is the difference between the first and second oxidation potentials.¹ We found organic metals (BEDT-ATD)₂X(THF) ($X = \text{PF}_6$, AsF_6 ; THF = tetrahydrofuran) which remain metallic down to 3 K.² In the previous paper, we assumed that these salts have one-dimension-like electronic properties only from the rather narrow ESR linewidths. Therefore, we carried out a band structure calculation to evaluate the dimensionality from the intermolecular transfer integrals. As a next strategy, we used smaller anions like a tetrahedral BF_4^- or solvent molecules like 2,5-dihydrofuran (DHF) instead of an octahedral PF_6^- anion or THF, in order to enhance intermolecular interactions by contraction of the crystal lattice. Contrary to our expectations, a metal-insulator (M-I) transition appeared in (BEDT-ATD)₂ BF_4 (THF) (hereafter named BF_4 (THF) salt) and (BEDT-ATD)₂ PF_6 (DHF) (named PF_6 (DHF) salt).

Here we report the band structure of (BEDT-ATD)₂ PF_6 (THF) (named PF_6 (THF) salt) and the experimental results of the structural, electrical and magnetic properties of BF_4 (THF) and PF_6 (DHF) salts. The possible origin of the M-I transition in the latter two salts is discussed from the viewpoint of the order-disorder transition of anions and solvent molecules.

EXPERIMENTAL

The black needle-like crystals of BF_4 (THF) and PF_6 (DHF) salts were grown by electrochemical oxidation in THF or DHF, respectively. X-Ray diffraction data were collected at room temperature with a Rigaku AFC-5R and an Enraf-Nonius CAD4

four-circle diffractometers. The crystal structures were solved by the direct method and refined by the full-matrix least-squares method using SHELXS 86 and teXsan softwares.^{3,4} The electrical conductivity was measured along the stacking direction with a conventional four-probe method using gold paste as a contact. The thermoelectric power was measured in a conventional apparatus by applying a small temperature difference of less than 0.5 K.⁵ ESR spectra were recorded on a Bruker ESP300E X-band spectrometer with an Oxford ESR900 cryostat. The spin susceptibility was calibrated with DPPH (diphenylpicrylhydrazyl) as a reference.

The electronic band structure of $\text{PF}_6(\text{THF})$ salt was calculated by the extended Hückel method and the tight-binding approximation.⁶

RESULTS

1 Band structure of $(\text{BEDT-ATD})_2\text{PF}_6(\text{THF})$

Figure 1 shows the donor sheet structure in $\text{PF}_6(\text{THF})$ salt. The overlap integral is largest ($A=5.57 \times 10^{-3}$) along the stacking direction. In addition, the crystal has a fairly large overlap integral ($q=-1.63 \times 10^{-3}$) along the transverse direction. The transfer integral t related to the overlap integral Q by $t=EQ$ (E being the energy of the highest occupied molecular orbital (HOMO) of ~ 10 eV) is evaluated to be $t_{\parallel} \sim 0.056$ eV along the intrastack direction and $t_{\perp} \sim 0.016$ eV along the interstack direction. The anisotropy of the transfer integral is relatively small ($|t_{\parallel}/t_{\perp}| \sim 3$).

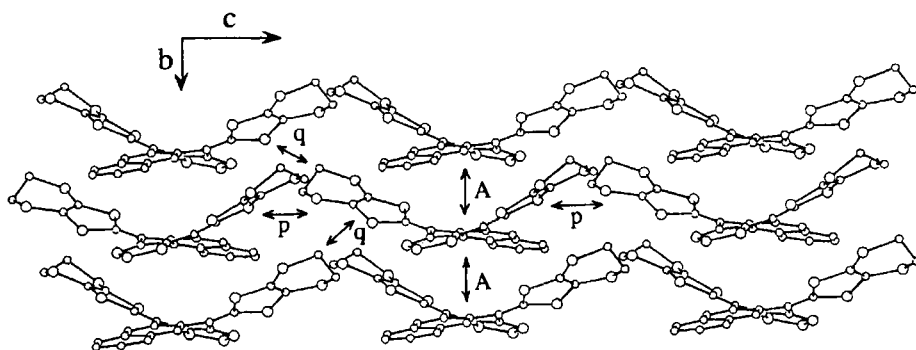


FIGURE 1 Molecular arrangement of BEDT-ATD molecules in a $(\text{BEDT-ATD})_2\text{PF}_6(\text{THF})$ crystal. The values of the overlap integral ($\times 10^{-3}$) are $A=5.57$, $p=0.15$ and $q=-1.63$.

Figure 2 shows the calculated band structure and Fermi surface. The band energy is dispersive along the intrastack direction Γ to Y and M to Z and along the interstack direction Z to Γ , so that the Fermi surface is nearly closed and slightly open along the c^* axis.

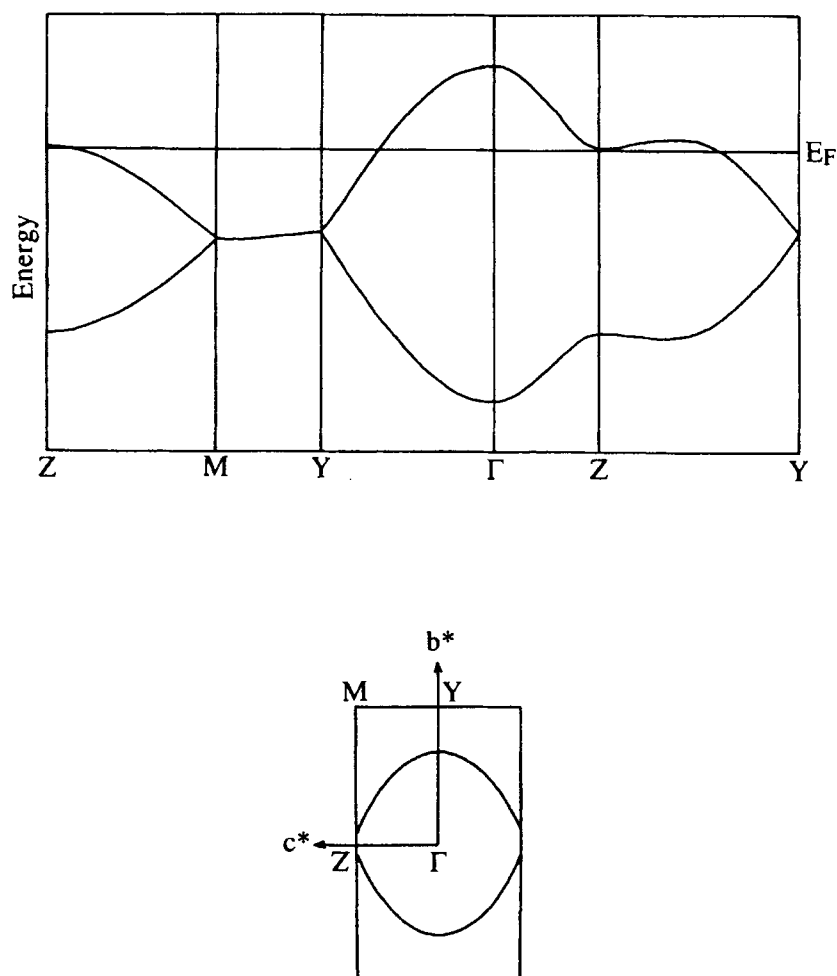


FIGURE 2 Band structure and Fermi surface of $(\text{BEDT-ATD})_2\text{PF}_6(\text{THF})$.

2 Physical properties of $(\text{BEDT-ATD})_2\text{BF}_4(\text{THF})$ and $(\text{BEDT-ATD})_2\text{PF}_6(\text{DHF})$

2.1 Crystal structure

Table I summarizes the crystal data of $\text{BF}_4(\text{THF})$ and $\text{PF}_6(\text{DHF})$ salts. Both salts are isostructural to $\text{PF}_6(\text{THF})$ salt.^{1,2} The crystal structure of $\text{BF}_4(\text{THF})$ salt is shown in Figures 3 (a) and (b). The nonplanar BEDT-ATD molecules are uniformly stacked along the b axis. The shortest interstack S...S distance (dotted line) is 3.69 Å for $\text{BF}_4(\text{THF})$ salt and 3.64 Å for $\text{PF}_6(\text{DHF})$ salt. These values are comparable to 3.66 Å in $\text{PF}_6(\text{THF})$ salt. The most significant difference is in the disordered state of anions and solvent molecules: In $\text{BF}_4(\text{THF})$ crystal, both BF_4^- anions and THF solvent molecules are disordered, while in $\text{PF}_6(\text{DHF})$ crystal, the PF_6^- anions are ordered and the DHF solvent molecules are disordered, similar to $\text{PF}_6(\text{THF})$ salt.

TABLE I Crystal data of $(\text{BEDT-ATD})_2\text{BF}_4(\text{THF})$ and $(\text{BEDT-ATD})_2\text{PF}_6(\text{DHF})$.

	$(\text{BEDT-ATD})_2\text{BF}_4(\text{THF})$	$(\text{BEDT-ATD})_2\text{PF}_6(\text{DHF})$
Crystal system	monoclinic	monoclinic
Space group	$P2_1/a$	$P2_1/a$
$a / \text{\AA}$	27.88(1)	27.801(1)
$b / \text{\AA}$	7.821(4)	7.904(1)
$c / \text{\AA}$	13.325(4)	13.280(1)
$\beta / ^\circ$	102.01(3)	103.66(1)
$V / \text{\AA}^3$	2842(4)	2835.6(3)
Z	2	2
$D_{\text{calc}} / \text{g cm}^{-3}$	1.63	1.70
R	0.136	0.048
No. of reflections	1025	4498
with $ F_o > 3\sigma F_o $		

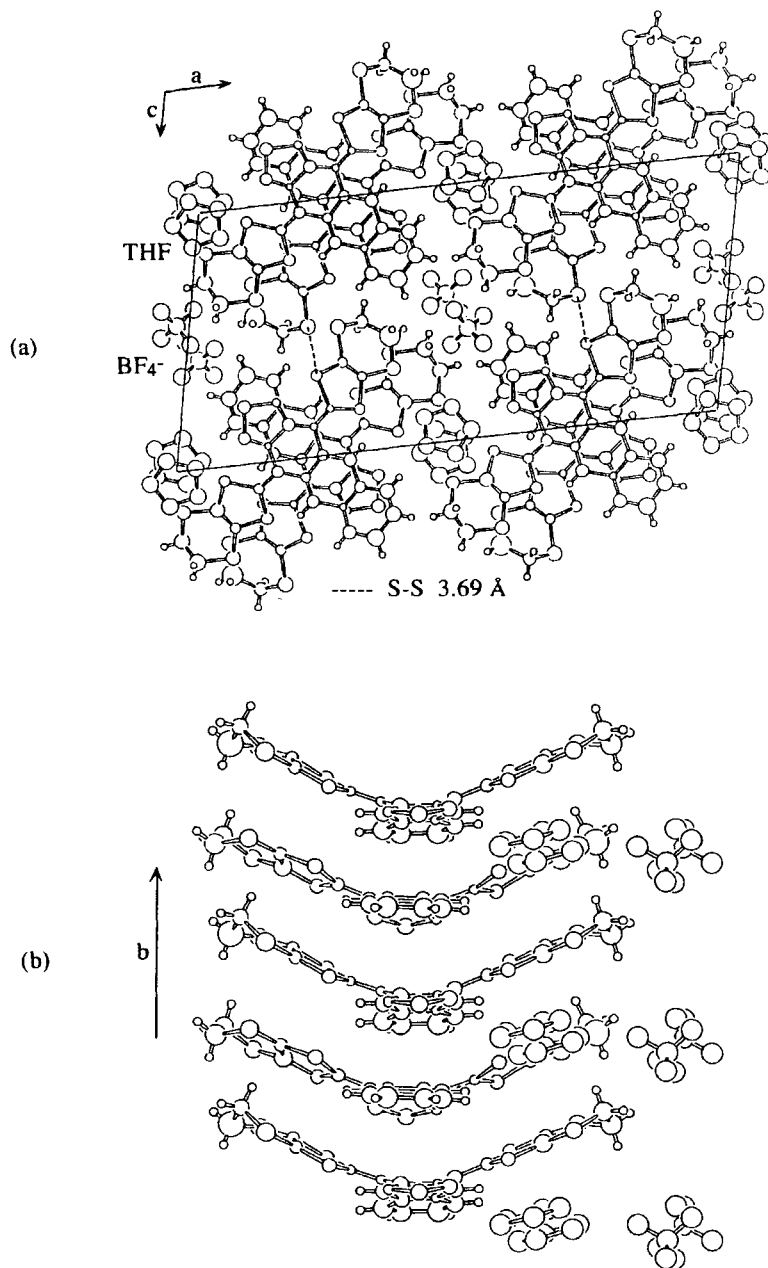


FIGURE 3 Crystal structure of $(\text{BEDT-ATD})_2\text{BF}_4(\text{THF})$: (a) Projection onto the ac plane, (b) Stacking of BEDT-ATD molecules along the b axis. The disordered BF_4^- anions and THF molecules are drawn as the nearest two molecules related by the inversion center.

2.2 Electrical resistivity

The resistivity of $\text{BF}_4(\text{THF})$ salt decreased gradually from $0.04 \text{ } \Omega\text{cm}$ at room temperature with decreasing temperature, indicating a metallic character. However $\text{BF}_4(\text{THF})$ crystal broke below $\sim 200 \text{ K}$. Fragility of the crystals seems to be common in the THF-including BEDT-ATD salts.²

On the contrary, $\text{PF}_6(\text{DHF})$ crystal did not break at low temperatures. Figure 4 shows the temperature-dependent resistivity of $\text{PF}_6(\text{DHF})$ salt. $\text{PF}_6(\text{DHF})$ salt also showed a resistivity of $0.04 \text{ } \Omega\text{cm}$ at room temperature and revealed a metal-like conduction down to around 150 K . Below 150 K the resistivity started to steeply increase, suggesting the occurrence of an M-I transition. The Arrhenius plot in the semiconducting region did not give a straight line, so that it was difficult to determine an activation energy from the resistivity measurement.

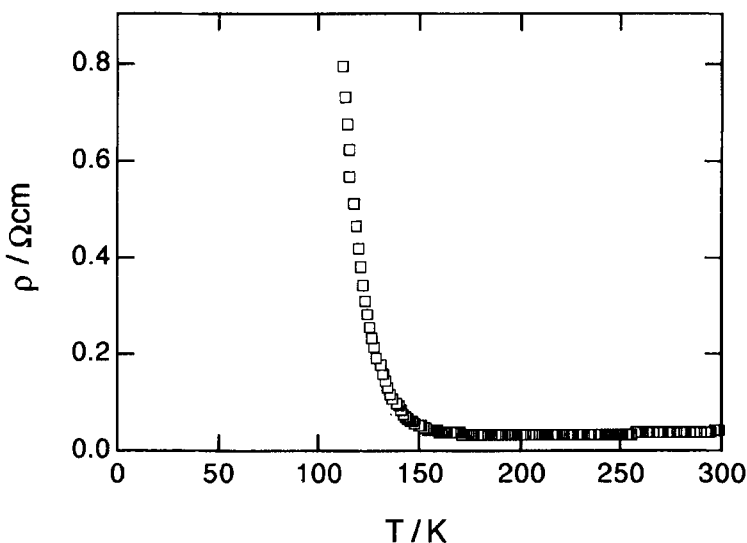


FIGURE 4 Temperature dependence of the electrical resistivity of $(\text{BEDT-ATD})_2\text{PF}_6(\text{DHF})$.

2.3 Thermoelectric power

The thermopowers at room temperature were $+48 \text{ } \mu\text{V K}^{-1}$ and $+47 \text{ } \mu\text{V K}^{-1}$ for $\text{BF}_4(\text{THF})$ salt and $\text{PF}_6(\text{DHF})$ salt, respectively. These values are in good agreement with $+47 \text{ } \mu\text{V K}^{-1}$ for $\text{PF}_6(\text{THF})$ salt. Since the thermopower of a metal depends on the

structure of the energy band at the Fermi energy, the same values of these three salts suggest the similarity of their band structures, as expected from the similar crystal structures of the three salts.

As shown in Figure 5, $\text{BF}_4(\text{THF})$ and $\text{PF}_6(\text{DHF})$ salts showed a metal-like linear-decrease of the thermopower in the high-temperature region. At low temperature, both salts underwent an M-I transition showing a gradual increase below ~ 200 K for $\text{BF}_4(\text{THF})$ salt and a steep increase below 150 K for $\text{PF}_6(\text{DHF})$ salt. The thermopower S for a semiconductor is given by

$$S = -\frac{k_B}{|e|} \left(\frac{r-1}{r+1} \cdot \frac{E_a}{k_B T} + \ln \frac{m_h}{m_e} \right),$$

where r is the ratio (μ_e/μ_h) of electron-to-hole mobility, E_a the activation energy, and m_h and m_e the effective masses of holes and electrons.⁷ In the present one-chain conductor, the condition of $\mu_h \gg \mu_e$ leads to $r=0$. If we plot the thermopower against the reciprocal temperature in the semiconducting region, the slope gives E_a . The values of E_a are obtained as 0.019 eV for $\text{BF}_4(\text{THF})$ salt and 0.024 eV for $\text{PF}_6(\text{DHF})$ salt.

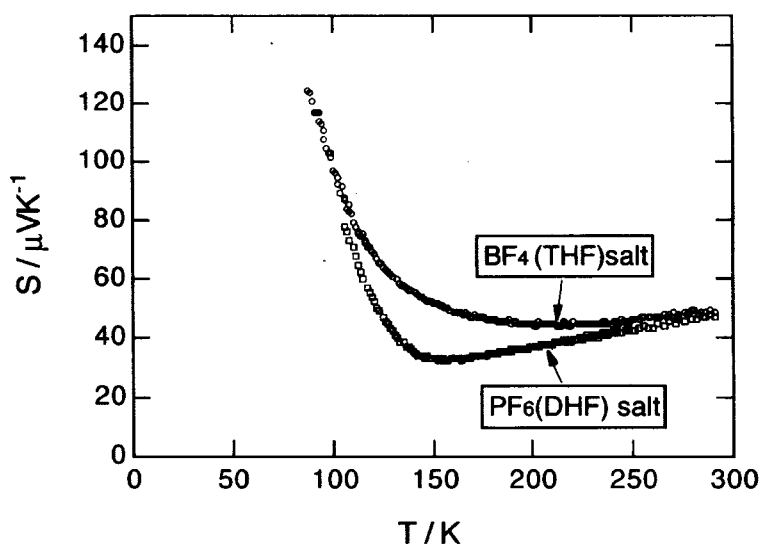


FIGURE 5 Temperature dependence of the thermoelectric power of $(\text{BEDT-ATD})_2\text{BF}_4(\text{THF})$ and $(\text{BEDT-ATD})_2\text{PF}_6(\text{DHF})$.

2.4 ESR

In the polycrystalline samples, $\text{BF}_4(\text{THF})$ salt showed a room-temperature ESR spectrum with $g=2.0053$ and linewidth $\Delta H=10.0$ G, whereas $\text{PF}_6(\text{DHF})$ salt showed $g=2.0055$ and $\Delta H=13.0$ G. In Figure 6, we present the temperature-dependent spin susceptibility of $\text{BF}_4(\text{THF})$ salt. The spin susceptibility (solid circles) after subtraction of the Curie component at low temperature was independent of temperature down to around 200 K, which can be attributed to the Pauli paramagnetic susceptibility. Then the susceptibility decreased exponentially, indicating an onset of an M-I transition accompanied by the transition from a triplet metallic state to a singlet ground state. The magnetic activation energy Δ is estimated to be 370 K (0.03 eV) for the expression $\chi=(C/T)\exp(-\Delta/T)$.⁸ This value is in good agreement with $E_a=0.02$ eV from the thermopower measurement.

$\text{PF}_6(\text{DHF})$ salt also showed an activation behavior with $\Delta=380$ K (0.03 eV) in the spin susceptibility below ~ 150 K which corresponds to the transition temperature observed in the transport measurements.

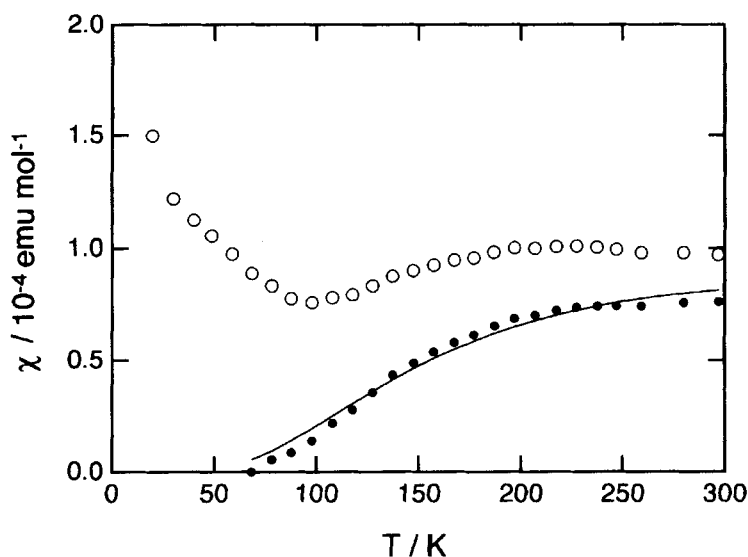


FIGURE 6 Temperature dependence of the spin susceptibility (open circles) of $(\text{BEDT-ATD})_2\text{BF}_4(\text{THF})$. The solid circles denote the susceptibility after subtraction of the Curie tail. The solid line corresponds to the calculated susceptibility for $\Delta=370$ K in the expression $\chi=(C/T)\exp(-\Delta/T)$.

DISCUSSION

The band structure calculation demonstrates that $\text{PF}_6(\text{THF})$ salt possesses a two-dimension-like electronic structure with a small anisotropy of the transfer integral and a nearly closed Fermi surface. In this crystal, the ethylenedithio groups are important to afford the transverse interactions. The two-dimensional network structure through the intermolecular $\text{S}\cdots\text{S}$ contacts of the ethylenedithio groups has been observed in many bis(ethylenedithio)tetrathiafulvalene (BEDT-TTF)-based organic metals.⁹ The stable metallic state at low temperature of $\text{PF}_6(\text{THF})$ salt will be better understood by considering the two-dimension-like nature which suppresses CDW (charge density wave) and SDW (spin density wave) instabilities inherent for pure one-dimensional metals.

The unit cell volume on replacing PF_6^- or THF by a smaller BF_4^- anion or a DHF solvent molecule remains almost unchanged, i.e. $V=2842 \text{ \AA}^3$ for $\text{BF}_4(\text{THF})$ salt and 2836 \AA^3 for $\text{PF}_6(\text{DHF})$ salt, compared with 2856 \AA^3 for $\text{PF}_6(\text{THF})$ salt. This means that the crystal structure is dominated by the arrangement of the bulky BEDT-ATD molecules, and the anion and solvent molecules occupy only the vacancies in between. However, such anion or solvent replacements have a great influence on the electronic state and introduce an M-I transition at 200 K for $\text{BF}_4(\text{THF})$ salt and 150 K for $\text{PF}_6(\text{DHF})$ salt.

Now we discuss a possible origin of the M-I transition. First we compare $\text{BF}_4(\text{THF})$ salt to $\text{PF}_6(\text{THF})$ salt. Though both salts have a similar crystal structure and metallic properties at room temperature, their low-temperature properties are quite different, where $\text{PF}_6(\text{THF})$ salt stays metallic and $\text{BF}_4(\text{THF})$ salt becomes insulating. The only difference between them is that noncentrosymmetric BF_4^- anions are disordered at room temperature. It is well known that the cation radical salts of tetramethyltetraselenafulvalene $[(\text{TMTSF})_2\text{X}]$ ($\text{X}=\text{tetrahedral anions such as } \text{ReO}_4^-, \text{BF}_4^- \text{ and } \text{ClO}_4^-$) undergo an M-I transition associated with an anion ordering at low temperature. The order-disorder transitions are observed at 177 K, 38 K and 24 K for $(\text{TMTSF})_2\text{ReO}_4$, $(\text{TMTSF})_2\text{BF}_4$ and $(\text{TMTSF})_2\text{ClO}_4$, respectively, by X-ray diffuse scattering and neutron diffraction.¹⁰⁻¹² The magnetic susceptibilities of $(\text{TMTSF})_2\text{X}$ salts decrease sharply like an SDW transition below the order-disorder transition temperature,^{13,14} whereas $\text{BF}_4(\text{THF})$ salt shows a CDW-like exponential decrease as shown in Figure 6. It is now puzzling to explain their different magnetic behavior.

Next we compare $\text{PF}_6(\text{DHF})$ salt to $\text{PF}_6(\text{THF})$ salt. THF is a single-bonded molecule with two conformations coming from a ring inversion motion. In $\text{PF}_6(\text{THF})$ salt, the THF molecules will remain disordered even at low temperature due to the ring

inversion motion, which prevents the order-disorder transition and stabilizes the metallic state. On the contrary, a DHF molecule has a double bond, which restricts the thermal motion. The DHF molecules may be more easily ordered at low temperature, which will give rise to the order-disorder transition. In the previous paper, we reported that $\text{PF}_6(\text{THF})$ salt reveals a pressure-induced M-I transition above 2.5 kbar.² The origin of the transition might be understood by supposing that the ring inversion motion of THF molecules is frozen under high pressure.

In addition, we obtained a crystal of $(\text{BEDT-ATD})_2\text{PF}_6(\text{DO})$, where DO stands for 1,3-dioxolane which includes two oxygen atoms. In this crystal, an M-I transition was observed at ~ 100 K in the electrical conductivity measurement. It seems that the solvent ordering is easier in the following sequence $\text{THF} < \text{DO} < \text{DHF}$. The M-I transition temperature also increases in the same order. Hence, $(\text{BEDT-ATD})_2\text{PF}_6(\text{Solvent})$ could be regarded as a new type of charge-transfer complexes in which the M-I transition can be changed by changing the solvent molecule.

We are now planning to study the X-ray diffraction of these systems at low temperature in order to get more insight into the superlattice structure associated with an anion or solvent molecule ordering.

DEDICATION

The authors would like to dedicate this article to Professor Yusei Maruyama who has made a huge contribution to the field of organic molecular crystals, conductors and superconductors on the occasion of his retirement celebration. We sincerely appreciate his encouragement and stimulation for the present work.

REFERENCES

1. Y. Yamashita, S. Tanaka and K. Imaeda, *Synth. Met.*, **71**, 1965 (1995).
2. K. Imaeda, Y. Yamashita, S. Tanaka and H. Inokuchi, *Synth. Met.*, **73**, 107 (1995).
3. G. M. Sheldrick, *Acta Crystallogr., Sect. A*, **46**, 467 (1990).
4. teXsan Single Crystal Structure Analysis Package, Molecular Structure Corporation, 1985; 1992.
5. P. M. Chaikin and J. F. Kwak, *Rev. Sci. Instrum.*, **46**, 218 (1975).
6. T. Mori, A. Kobayashi, Y. Sasaki, H. Kobayashi, G. Saito and H. Inokuchi, *Bull. Chem. Soc. Jpn.*, **57**, 627 (1984).
7. P. M. Chaikin, R. L. Greene, S. Etemad and E. Engler, *Phys. Rev. B*, **13**, 1627 (1976).

8. Y. Tomkiewicz, B. A. Scott, L. J. Tao and R. S. Title, *Phys. Rev. Lett.*, **32**, 1363 (1974).
9. H. Kobayashi, A. Kobayashi, Y. Sasaki, G. Saito, T. Enoki and H. Inokuchi, *J. Am. Chem. Soc.*, **105**, 297 (1983); H. Kobayashi, T. Mori, R. Kato, A. Kobayashi, Y. Sasaki, G. Saito and H. Inokuchi, *Chem. Lett.*, **1983**, 581.
10. R. Moret, J. P. Pouget, R. Comès and K. Bechgaard, *Phys. Rev. Lett.*, **14**, 1008 (1982).
11. J. P. Pouget, G. Shirane, K. Bechgaard and J. M. Fabre, *Phys. Rev. B*, **27**, 5203 (1983).
12. P. C. W. Leung, A. J. Schultz, H. H. Wang, T. J. Emge, G. A. Ball, D. D. Cox and J. M. Williams, *Phys. Rev. B*, **30**, 1615 (1984).
13. H. J. Pedersen, J. C. Scott and K. Bechgaard, *Phys. Rev. B*, **24**, 5014 (1981).
14. C. S. Jacobsen, H. J. Pedersen, K. Mortensen, G. Rindorf, N. Thorup, J. B. Torrance and K. Bechgaard, *J. Phys. C: Solid State Phys.*, **15**, 2651 (1982).